OPEN

Citation: Cell Death and Disease (2014) 5, e1144; doi:10.1038/cddis.2014.110

www.nature.com/cddis

MiR-19a/b modulate the metastasis of gastric cancer cells by targeting the tumour suppressor MXD1

Q Wu[1,2], Z Yang[1,2], Y An[1,2], H Hu[1], J Yin[1], P Zhang[1], Y Nie[1], K Wu[1], Y Shi*[,1] and D Fan*[,1]

The microRNAs 19a and 19b, hereafter collectively referred to as miR-19a/b, were recognised to be the most important miRNAs in the oncomiRs–miR-17-92 cluster. However, the exact roles of miR-19a/b in cancers have not been elucidated. In the present study, miR-19a/b was found to be over-expressed in gastric cancer tissues and significantly associated with the patients' metastasis of gastric cancer. Using gain or loss-of-function in *in vitro* and *in vivo* experiments, a pro-metastatic function of miR-19a/b was observed in gastric cancer. Furthermore, reporter gene assay and western blot showed that MXD1 is a direct target of miR-19a/b. Functional assays showed that not only MXD1 had an opposite effect to miR-19a/b in the regulation of gastric cancer cells, but also overexpression of MXD1 reduced both miR-19a/b and c-Myc levels, indicating a potential positive feedback loop among miR-19a/b, MXD1 and c-Myc. In conclusion, miR-17-92 cluster members miR-19a/b facilitated gastric cancer cell migration, invasion and metastasis through targeting the antagonist of c-Myc – MXD1, implicating a novel mechanism for the malignant phenotypes of gastric cancer.

Cell Death and Disease (2014) **5,** e1144; doi:10.1038/cddis.2014.110; published online 27 March 2014
Subject Category: Cancer

MicroRNAs (miRNAs) are small, non-coding RNAs 19–24 nucleotides in length that act in association with the RNA-induced silencing complex to regulate expression of multiple genes by either inducing translational silencing or causing degradation of the mRNA of the targeted genes.[1,2] It has been firmly recognised that miRNAs regulate many key cellular processes, such as cell growth, cell cycle, differentiation and cell death. Understanding miRNA functions and transcriptional regulatory circuits requires elucidation of the molecular pathways that are responsible for specific biological phenomenon through the integration of transcription factors, miRNAs and the direct targets of miRNAs.[3]

More recently, miRNAs have emerged as oncogenes or tumour suppressors[4] that act as central players in networks that establish regulatory circuits in cancers. The miR-17-92 cluster, one of the miRNA clusters transcriptionally activated by the proto-oncogene c-Myc,[5] first attracted attention following a series of observations that linked these miRNAs to cancer pathogenesis; the miR-17-92 cluster was shown to be over-expressed in many cancers, including lung, colon and breast cancer and neuroblastoma.[6–9] An important role for these miRNAs in the regulatory circuit that controls cellular life and the cell cycle further illustrates the contributions of these miRNAs to tumorigenesis. Specifically, the transcriptional activators E2F1 and E2F3 can directly activate the transcription of miR-17-92, and, in turn, E2F1, E2F2 and E2F3 are among the first experimentally verified targets of these miRNAs.[10]

Although the miR-17-92 cluster members have been established as oncomiRs, their oncogenic contributions in cancers have not been assigned. The miR-17-92 cluster contains six members: miR-19a/b, miR-17/20a, miR-18a and miR-92a. We chose miR-19a/b for the present study because they were recently identified to be the most important miRNAs in this cluster,[11,12] and we observed a pro-metastatic function of miR-19a/b in our primary studies. Expression of miR-19a/b was previously found to be correlated with lymph node metastasis in non-small cell lung cancer patients,[13] however, the exact roles of miR-19a/b in cancer metastasis have not been elucidated. In the present study, we aimed at exploring the relationships between miR-19a/b and metastasis, and the potential mechanisms. Using gain and loss-of-function assays, a pro-metastatic function of miR-19a/b was observed. Furthermore, the tumour suppressor MXD1 was demonstrated to be a direct target of miR-19a/b. Our findings provide mechanistic insight into the function of miR-19a/b and have important implications for understanding gastroenterological disorders resulting from altered regulation of miRNA pathways.

Results

Expression of miR-19a/b was associated with metastasis in gastric cancer patients. miR-19a/b were previously regarded as oncomiRs and were detected to regulate the self-renewal of gastric cancer stem cells in our department

[1]State Key Laboratory of Cancer Biology and Xijing Hospital of Digestive Diseases, Xijing Hospital, Fourth Military Medical University, Xi'an, China
*Corresponding authors: Y Shi or D Fan, State Key Laboratory of Cancer Biology and Xijing Hospital of Digestive Diseases, Xijing Hospital, Fourth Military Medical University, Chang Le West Road, Xi'an, Shaanxi 710032, China. Tel: +86 29 84771501; Fax: +86 29 82539041; E-mail: shiyquan@fmmu.edu.cn or daimingfan@fmmu.edu.cn
[2]These authors contributed equally to this work.
Keywords: MiR-19; MXD1; metastasis; gastric cancer
Abbreviations: miRNA, microRNA; MXD1, MAX dimerisation protein 1; RISC, RNA-induced silencing complex; E2F1, E2F transcription factor 1; E2F2, E2F transcription factor 2; E2F3, E2F transcription factor 3; HR, hazard ratio; EGFP, enhanced green fluorescent protein; 3′ UTR, 3′ untranslated region; AS, antisense; MAX, MYC associated factor X
Received 13.12.13; revised 13.2.14; accepted 14.2.14; Edited by A Stephanou

(data not shown). We firstly tested the expression of miR-19a/b in gastric cancer tissues by real-time PCR using RNAs from 141 patients who underwent gastrectomy and were followed up at Xijing Hospital during 2006–2008. We used a $\log 2^{-\Delta\Delta Ct}$ analysis to statistically describe the expression levels of miR-19a/b. As shown in Figures 1a and b, the results verified that the expression of miR-19a (A) or miR-19b (B) was higher in 10 of 15 or 10 of 15 randomly selected human gastric cancer tissues, respectively, compared with the adjacent normal tissues. Interestingly, there was 13 out of 15 gastric cancer samples with either miR-19a or miR-19b overexpression from the results of the real-time PCR (Figures 1a and b). Correlations between miR-19a/b expression levels and clinicopathologic characteristics of gastric cancer are summarised in Table 1. A statistically significant association between miR-19a/b expression levels and metastasis of gastric cancer patients was observed in this study. The expression of miR-19a or miR-19b in gastric cancer patients did not correlate with age, gender or cell differentiation, but correlated with remote metastasis of gastric cancer patients ($P<0.001$). The expression of miR-19a was also significantly associated with TNM stage and lymph node metastasis ($P<0.001$).

To examine whether the expression levels of miR-19a/b were associated with survival in the above gastric cancer patients, we ranked the patients on the basis of the relative

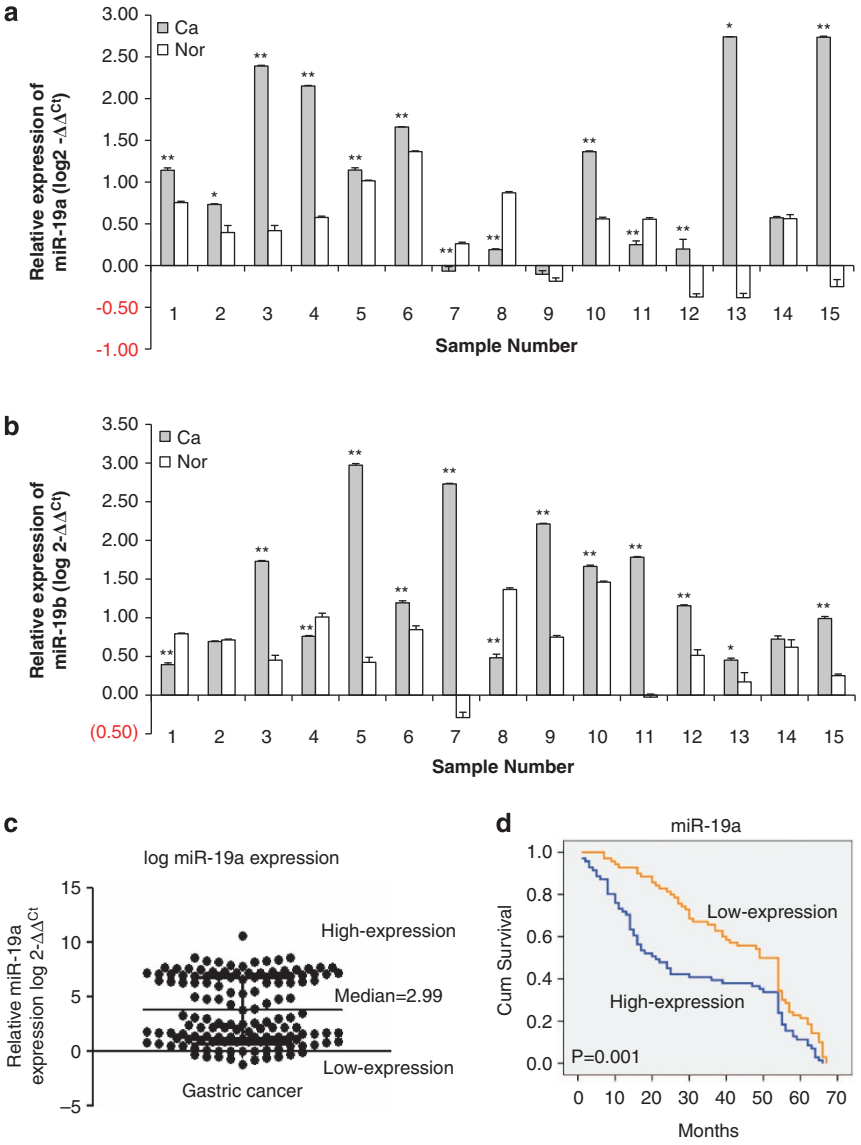

Figure 1 Expression of miR-19a/b in gastric cancer tissues and their association with clinicopathologic characteristics. (**a** and **b**) Real-time PCR shows the expression of miR-19a (**a**) and miR-19b (**b**) in 15 randomly selected gastric cancer samples compared with the adjacent normal tissues (**$P\leq0.01$, *$P\leq0.05$). Each experiment was independently repeated at least three times. Error bars correspond to the mean ± S.D. (**c**) Gastric cancer samples were divided into two groups, according to the median expression of miR-19a (median = 2.99). Cases with levels of miR-19a below the mean were considered miR-19a low expressers ($n=70$), and those with levels of miR-19a above the mean were considered miR-19a high expressers ($n=70$). (**d**) Kaplan–Meier survival curve and log-rank test for gastric cancer patients between high and low miR-19a expressers to evaluate the relationship with patient survival

Table 1 Association of miR-19a/b expression with clinicopathologic characteristics

Variables	No. of cases (%)	Expression of miR-19a		Expression of miR-19b	
		Mean ± S.D.	*P*-value	Mean ± S.D.	*P*-value
Age (years)					
≥60	72 (51%)	3.93 ± 3.03	0.57	1.55 ± 1.03	0.44
<60	69 (49%)	3.64 ± 3.04		1.40 ± 1.22	
Gender					
Male	103 (73%)	3.84 ± 3.05	0.74	1.44 ± 1.04	0.54
Female	38 (27%)	3.65 ± 2.99		1.57 ± 1.33	
Degree of differentiation					
Well and moderately differentiated	46 (33%)	3.19 ± 2.89	0.11	1.45 ± 0.82	0.83
Poorly differentiated	95 (67%)	4.08 ± 3.07		1.49 ± 1.25	
TNM stage					
Stage I/II	67 (48%)	2.26 ± 2.49	<0.001	1.31 ± 0.99	0.09
Stage III/IV	74 (52%)	5.18 ± 2.81		1.63 ± 1.22	
Lymph node metastasis					
Yes	86 (61%)	4.81 ± 2.92	<0.001	1.57 ± 1.20	0.20
No	55 (39%)	2.19 ± 2.48		1.32 ± 0.98	
Remote metastasis					
Yes	21 (15%)	6.96 ± 2.50	<0.001	2.20 ± 1.90	<0.001
No	120 (85%)	3.23 ± 2.77		1.35 ± 0.88	

expression levels obtained via real-time PCR and divided them into high-expression group and low-expression group using the 50th percentile (median) as the cut-off point (Figure 1c). HR from the univariate Cox regression analysis showed that the TNM stage and the expression of miR-19a was correlated with death from any cause (Figure 1d, $P=0.001$). A multivariate Cox regression analysis identified the level of miR-19a as an independent factor that was associated with overall survival (Supplementary Table 1).

Stable overexpression of miR-19a/b miRNAs promoted gastric cancer cell migration and invasion *in vitro*. Because miR-19a/b were over-expressed in gastric cancer tissues compared with normal tissues and their expression was associated with the metastasis of gastric cancer patients, we speculated that the overexpression of miR-19a/b might promote the migratory and invasive abilities of gastric cancer cells. To test the metastatic ability of miR-19a/b, we constructed an EGFP-expressing lentivirus with miR-19a/b precursors or a negative control small RNA and infected them into gastric cancer cell lines SGC7901 and MKN28. The EGFP-positive cells were detected using fluorescence microscopy and were sorted using a FACS machine as indicated in Supplementary Figures 1A and B. After sorting for EGFP-positive cells, the overexpression of mature miR-19a/b was confirmed by real-time PCR as shown in Figures 2a and b. The SGC7901 and MKN28 cells infected with lenti-miR-19a/b showed pro-migratory ability compared with the lenti-NC infection group (Figure 2c). Similar results were observed in cell invasion assays as indicated in Figure 2d.

To avoid the cross reaction of miR-19a and miR-19b, we performed real-time PCR of miR-19a/b in miR-19a and miR-19b-stable over-expressing cells. As shown in Supplementary Figure 3A, miR-19b expression did not increase in miR-19a-stable over-expressing cells compared with the NC group ($P>0.05$). Also, the miR-19a expression did not change in miR-19b over-expressing cells compared with the NC group as shown in Supplementary Figure 3B ($P>0.05$).

Transient transfection of miR-19a/b precursors and inhibitors regulated gastric cancer cell migration and invasion *in vitro*. To avoid the experimental artefacts with regard to cellular changes induced by the stable infection of the lentiviral constructs, we further purchased commercial miR-19a/b precursors and inhibitors from Applied Biosystems (Invitrogen, Carlsbad, CA, USA). We performed transient transfection of SGC7901 and MKN28 gastric cancer cell lines using a siPORT NeoFX Transfection Agent (Invitrogen) with miR-19a/b precursors and inhibitors. The transient transfection efficiency was detected by real-time PCR (Supplementary Figures 2A and B, Figures 3a and b). Consistent with the stable transfection results, the transient transfection of miR-19a or miR-19b precursors significantly increased the migration and invasion abilities of gastric cancer cells (Supplementary Figures 2C and D), while the inhibitors remarkably impeded cell migration and invasion *in vitro* (Figures 3c and d).

miR-19a/b stably over-expressing cells were prone to metastasise in nude mice. To test the *in vivo* relationships between miR-19a/b and metastasis, we performed a caudal vein injection using cells stably expressing miR-19a/b in BALB/C nude mice. To facilitate the detection of metastasis, a luciferase-labelled SGC7901Luc cell line established in our lab was infected with lenti-miR-19a, lenti-miR-19b miRNAs or the negative control lentivirus (cells named SGC7901Luc-19a, SGC7901Luc-19b or SGC7901Luc-NC, respectively). The luciferase signals of SGC7901Luc cells and the

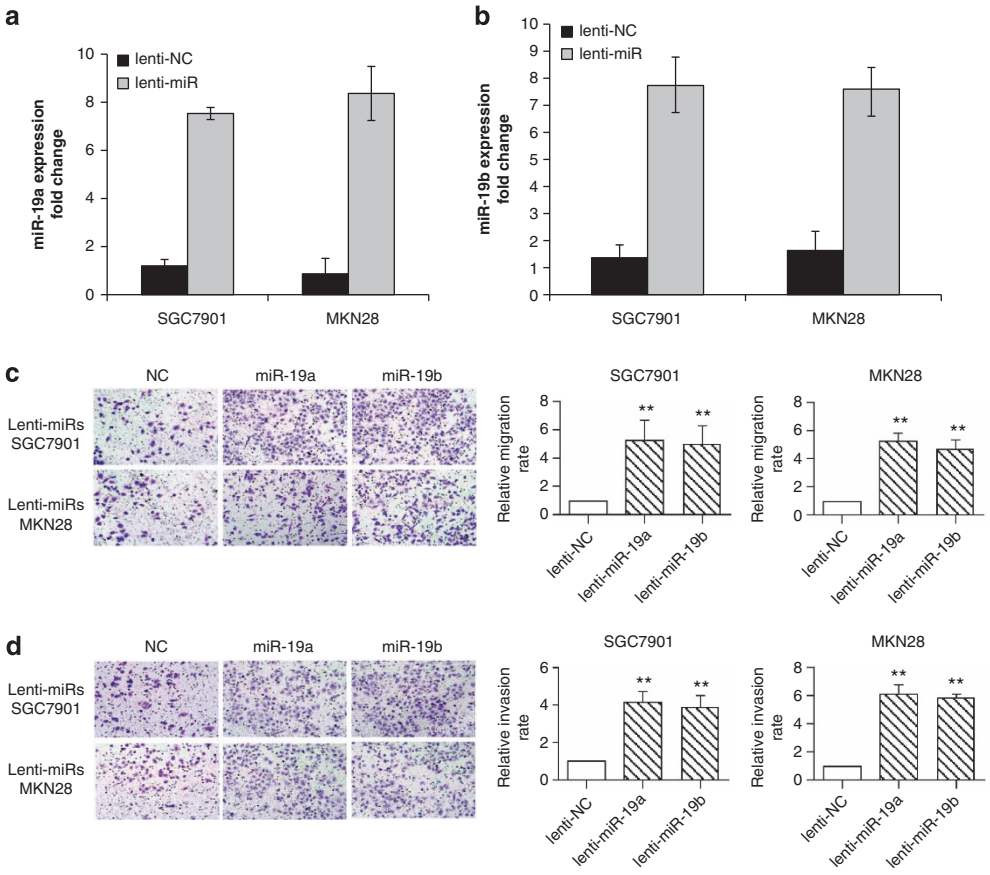

Figure 2 miR-19a/b miRNAs were stably over-expressed in gastric cancer cell lines SGC7901 and MKN28 by lentiviral infection. Overexpression of miR-19a/b promoted gastric cancer cell migration and invasion. (**a** and **b**) Successful stable overexpression of miR-19a/b in gastric cancer cell lines SGC7901 and MKN28 was confirmed by real-time PCR. Fold change was used to calculate each of the values of miR-19a/b relative to the negative control. Each experiment was repeated at least three times. Error bars correspond to the mean ± S.D. (**c**) Representative images of migrated cells on transwell plates that were originally plated with 10^5 cells; the number of migrated cells is indicated (**$P<0.01$, *t*-test). Each experiment was repeated at least three times. Error bars correspond to the mean ± S.D. (**d**) Representative images show cells invaded through transwell coated with matrigel and the invaded cell numbers. In the upper chambers, 5×10^5 cells were plated and incubated for 24 h at 37 °C. Cells invaded through to the downside of the membrane, were fixed with 100% methanol and stained with 0.2% crystal violet (**$P<0.01$ compared with the NC group, *t*-test). Each experiment was repeated at least three times. Error bars correspond to the mean ± S.D.

gradient-diluted cells are shown in Supplementary Figure 1C. The successful overexpression of mature miR-19a/b miRNAs was confirmed by real-time PCR (Figure 4a). Two weeks later, only two of six mice in the lenti-miR-19a group showed slight signals in the lungs (Figure 4b). Seven weeks after injection, all six mice in the SGC7901Luc-19a and SGC7901Luc-19b group showed metastases in the lungs or livers (Figure 4c, Supplementary Table 2). On the contrary, only two out of six of the mice injected with SGC7901Luc-NC cells had lung or liver metastases as shown in Figures 4c and d. Furthermore, the luciferase signals of tumours in the lungs of the SGC7901Luc-19a and SGC7901Luc-19b groups were much higher than the SGC7901Luc-NC group (Figure 4d). The number of nude mice with metastasis in the liver or lung in each group are shown in Supplementary Table 2. At the end of the experiment, the nude mice were sacrificed, and the lungs and livers of the nude mice were harvested, fixed and embedded in paraffin for further staining. The formation of tumours in the lungs and livers was further confirmed by H&E staining as indicated in Figure 4e.

miR-19a/b miRNAs targeted MXD1 transcript by binding the 3′ UTR of MXD1 transcripts. *In silico* analysis using miRanda software (http://www.microrna.org/microrna/home.do) showed that the 3′-UTR of human MXD1 contains two conserved putative target sites for miR-19a/b miRNAs (Figure 5a). To validate these target sites, the 3′-UTR of human MXD1 was amplified and inserted in both orientations downstream of the luciferase gene in the pGL3-control vector, generating sense (S) and antisense (AS) constructs, collectively referred to as Luc-1 in Figure 5a. Two shorter clones (Luc-2 and Luc-3) were prepared similarly (Figure 5a). The transfection of SGC7901 cells with miR-19a or miR-19b precursors significantly decreased the expression of Luc-1S while having no effect on Luc-1AS expression (Figure 5b). In contrast, no affect was observed in cells transfected with miR-150, in accordance with the fact that the MXD1 3′-UTR does not contain a miR-150 target site (Figure 5b). The expression of Luc-2S was also reduced by either miR-19a or miR-19b precursors but not miR-150 (Figure 5c). Furthermore, miR-19a and miR-19b targeted Luc-3S but not Luc-3AS, as indicated in Figure 5d.

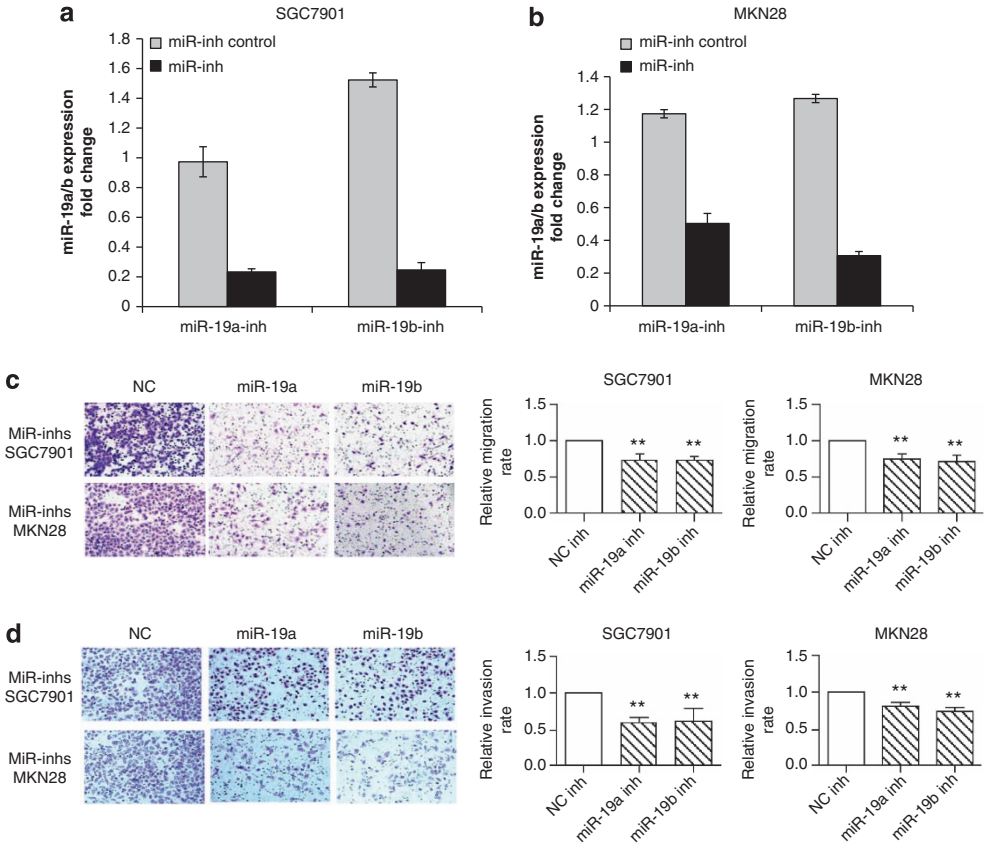

Figure 3 miR-19a/b miRNA inhibitors (inhs) were transiently transfected in gastric cancer cell lines SGC7901 and MKN28. Inhibition of miR-19a/b expression impeded gastric cancer cell migration and invasion. (**a** and **b**) Transient transfections of miR-19a/b inhibitors and miR-inhibitor control (NC inh) were performed using the dosage of 150 nM RNAs. Inhibition of miR-19a/b in gastric cancer cells was confirmed by real-time PCR 48 h after transfection. Each experiment was repeated at least three times. Error bars correspond to the mean ± S.D. (**c**) Representative images show migrated cells on transwell plates originally plated with 10^5 cells and the number of migrated cells using cells transiently transfected with miR-19a/b inhs and NC (**$P<0.01$ compared with NC group, *t*-test). Each experiment was repeated at least three times. Error bars correspond to the mean ± S.D. (**d**) Representative images show that cells invaded through transwell coated with matrigel and the invaded cell numbers after transient transfection of miR-19a/b inhs and NC. In the upper chambers, 5×10^5 cells were plated and incubated for 24 h at 37 °C. Cells invaded through to the downside of the membrane, were fixed with 100% methanol and stained with 0.2% crystal violet (**$P<0.01$ compared with the NC group, *t*-test). Each experiment was repeated at least three times. Error bars correspond to the mean ± S.D.

Overexpression of MXD1 without 3′ UTR-impaired miR-19a/b effects. To determine the downregulating effects of miR-19a/b at the protein level, we performed western blotting assays using an anti-MXD1 antibody. As expected, the transient transfection of SGC7901 cells with pre-miR-19a or pre-miR-19b decreased MXD1 levels (Figure 5e), while cells transiently transfected with miR-19a or miR-19b inhibitors showed increased MXD1 levels, which suggest that miR-19a/b miRNAs regulate MXD1 expression *in vivo* at the post-transcriptional level.

To further confirm that MXD1 is a target of miR-19a and miR-19b, we performed real-time PCR using RNAs from the 15 paired malignant and normal tissues. As shown in Figures 6a and b, expression of MXD 1 adversely correlated with both the expression of miR-19a (A, $P=0.001$) and miR-19b (B, $P=0.009$).

To further prove that MXD1 is the major player downstream of miR-19a/b, we performed migration assay using cells transfected with pre-NC, pre-miR-19a, pre-miR-19a and MXD1 without 3′UTR, pre-miR-19b, pre-miR-19b and MXD1 without 3′UTR. The results showed that cotransfection of MXD1 without 3′UTR, restricted the effects of pre-miR-19a or pre-miR-19b transfection alone as indicated in Figures 6c and d. In another word, the overexpression of miR-19a/b was rescued by overexpression of MXD1 without 3′UTR.

Overexpression of MXD1 repressed c-Myc and miR-19a/b levels and impeded the malignant phenotypes of gastric cancer cells. It was previously reported that MXD1 can compete with c-Myc for interaction with MAX and has an opposite role to c-Myc in the regulation of the growth of human tumour cells. To test c-Myc expression and MXD1 function in gastric cancer cells when MXD1 is over-expressed, we constructed an HA-tagged MXD1. As indicated in Figure 7a, western blot showed that the c-Myc level was reduced in cells transfected with HA-MXD1. *In vitro* migration and invasion assays (Figures 7b and c) showed that HA-MXD1 impeded migration and invasion abilities of gastric cancer cells, while si-MXD1 promoted migration and invasion compared with the vector control group. MTT assays indicated that MXD1 decreased the growth speed of SGC7901 cells, while si-MXD1 promoted proliferation in

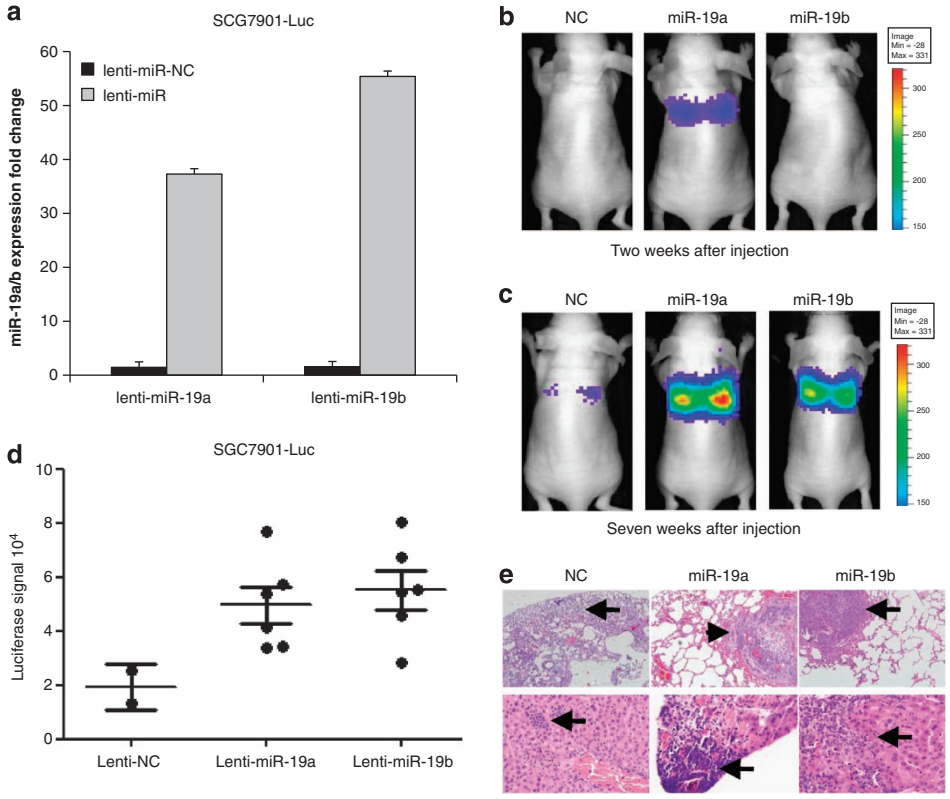

Figure 4 Stable overexpression of miR-19a/b promoted gastric cancer cell metastasis in BALB/C nude mice. Lenti-miR-19a/b miRNAs were stably infected in the firefly luciferase-labelled SGC7901 cells (SGC7901Luc). (**a**) Successful overexpression of mature miR-17-92 in SGC7901Luc was confirmed by real-time PCR. Relative fold change was used to calculate each of the values of miR-17-92 relative to the negative control. Each experiment was repeated at least three times. Error bars correspond to the mean ± S.D. (**b**) Representative images of mice two weeks after injection under the IVIS 100 system (Xenogen, Hopkinton, MA, USA). (**c** and **d**) Representative images show luciferase intensity in the lungs of mice seven weeks after injection (**c**) and the luciferase signals detected (**d**) ($P<0.05$ compared with lenti-NC infected cells, *t*-test). Error bars correspond to the mean ± S.D. (**e**) Hematoxylin and eosin staining (HE staining) of the lung (× 100) and the liver (× 400) of mice injected with 2×10^6 cells into the caudal vein. Arrows indicate focal metastasis

gastric cancer cells (Figure 7d). Our results demonstrated that MXD1 has an antimigratory, anti-invasive and antiproliferative function in gastric cancer. Moreover, the present study demonstrated that as the target gene of the oncomiRs miR-19a/b, MXD1 has a tumour-suppressive effect in gastric cancer cells.

To test whether miR-19a and miR-19b levels were regulated by MXD1, we performed real-time PCR on MXD1 over-expressing cells or cells transfected with MXD1 siRNAs (si-MXD1). As shown in Figures 7e and f, in MXD1 over-expressing cells, the expression levels of miR-19a and miR-19b were two or threefold lower than in the vector control group (Figure 7e). In si-MXD1 expressing cells, miR-19a and miR-19b expression levels were three to four times higher compared with the vector control group (Figure 7f). These results demonstrated that although miR-19a/b can down-regulate MXD1 expression by binding its 3′ UTR, over-expression of MXD1 can also reduce miR-19a/b expression levels, indicating a potential miRNA target gene self-regulatory loop between miR-19a/b and MXD1.

Discussion

The human miR-17-92 cluster is located on 13q31.3, a frequently amplified locus in colorectal cancers and lymphomas. The miR-17-92 cluster members, including miR-17/20a, miR-19a/b, miR-18a and miR-92a, were identified to be over-expressed in many cancers, including breast,[6] lung,[7] pancreatic,[14] colon[8] and gastric cancer.[15,16] Each member of the cluster is predicted to regulate a variety of different cellular targets; however, the functions of miRNAs in this cluster were still unclear. He L *et al.*[17] originally identified the miR-17-92 cluster as a potential human oncogene in B-cell lymphomas. Later, O Donnell *et al.*[5] demonstrated the transcriptional activation of the miR-17-92 cluster by the proto-oncogene c-Myc, thus establishing a potential role of this cluster in cell proliferation, growth and apoptosis. Recently, Mu *et al.*[11] identified miR-19a/b as the most important miRNAs of this cluster. Using deletion-reintroduction mouse models, they found that reintroduction of miR-19a/b rescued oncogenicity but not to the same extent as reintroduction of the entire cluster, indicating the pro-tumourigenic activity within this cluster. Using gain-of-function models, Olive *et al.*[12] also found that overexpression of the full cluster without miR-92 enhanced tumorigenesis, but when miR-19a and miR-19b were lost from the cluster, tumorigenesis was not enhanced, indicating the important function of miR-19 in tumorigenesis.

Although miR-19a and miR-19b were found to be the most significant miRNAs of the miR-17-92 cluster, and were

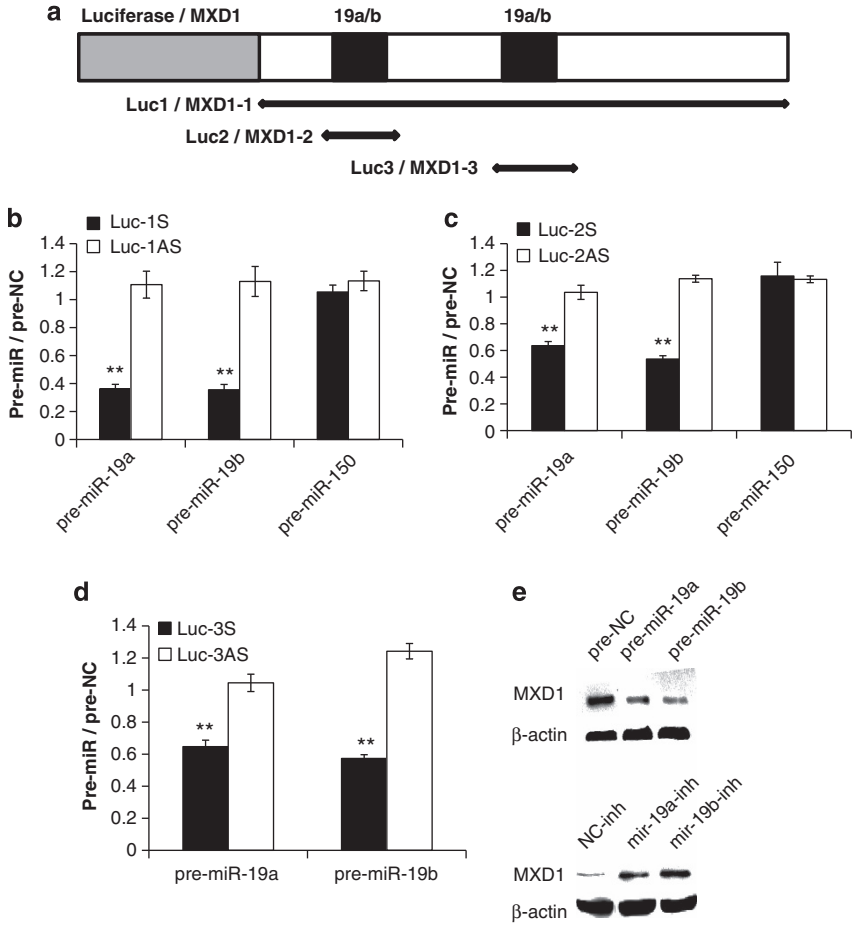

Figure 5 MXD1 transcripts were direct targets of miR-17-92 miRNAs. (**a**) Schematic representation of MXD1 3′-UTR constructs in pGL3-Control (Luc-1,-2,-3). Conserved putative target sites for miR-19a/b miRNAs were indicated. 19a, 19b and 19a/b in the figures mean miR-19a, miR-19b and miR-19a/b, respectively. (**b–d**) Luciferase assays were performed with Luc-1(B), Luc-2(C) and Luc-3(D) as indicated, both in sense (S) and antisense (AS) orientations. Bars indicate the ratios of the firefly luciferase (normalised to Renilla luciferase) activity measured following transfection with miR-19a/b pre-miRNAs to that obtained following transfection with the pre-miR control (pre-NC) for the same construct (**$P<0.01$, compared with the AS group, *t*-test). Each experiment was repeated at least three times. Error bars correspond to the mean ± S.D. (**e**) Western blot showing the changes in MXD1 protein levels after transient transfection of miR-19a/b precursors or inhibitors

reported to have a broad and significant roles in normal or abnormal cells of human body,[18–21] the exact function and the potential mechanisms of them in gastric cancer has not been fully clarified. We have previously found that the expression of the miR-17-92 cluster members were gradually changed during the differentiation of gastric cancer stem cells, among the six members, miR-19b/20a/92a can regulate the self-renewal of gastric cancer stem cells through activating the Wnt-β-catenin signalling.[22] Further study found that miR-19a/b could sustain the multi-drug resistance of gastric cancer cells.[23] In the present study, we first observed that miR-19a/b was over-expressed in most of the randomly selected gastric cancer samples and overexpression of miR-19a and miR-19b was significantly associated with metastasis in gastric cancer patients. Furthermore, *in vivo* and *in vitro* experiments were performed to test the relationships between miR-19a/b miRNAs and metastasis in gastric cancer using both stable and transient miR-19a/b expressing cells. Moreover, a pro-migratory, pro-invasive and pro-metastatic effect was observed in this study using *in vitro* and *in vivo* metastatic assays, which was consistent with the previous studies that the miR-17-92 cluster acts as oncomiRs in cancers.

The c-Myc onco-protein is currently viewed as an important regulator that stimulates cell growth and proliferation in response to extra-cellular signals. C-Myc binds to specific DNA sequences and affects the transcription of multiple genes involved in protein synthesis, cell cycle and proliferation. A recent study confirmed the direct binding of c-Myc to the miR-17-92 promoter regions on chromosome13, indicating the transcriptional activation of miR-17-92 by c-Myc. As an antagonist of c-Myc, MXD1 was known to modulate c-Myc function by competing with c-Myc for interaction with Max,[24] the obligatory partner of c-Myc for almost all its biological functions. Additionally, MXD1 and c-Myc proteins were found to have contrasting roles in human tumour cells;[25] c-Myc increased cell growth, decreased cell doubling time and reduced cell-cycle time, while MXD1 exerted the opposite effects. In the present study, we demonstrated that MXD1 was directly targeted by miR-19a and miR-19b miRNAs as these miRNAs could bind the 3′ UTR

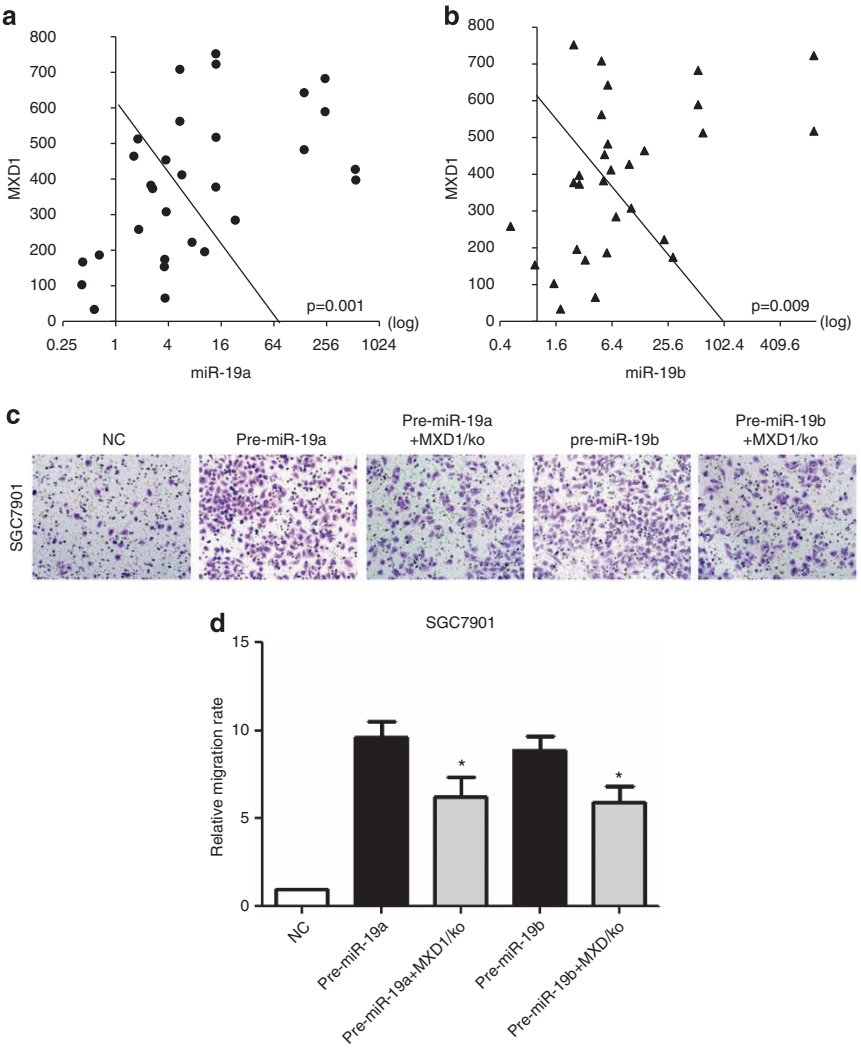

Figure 6 Overexpression of MXD1 without 3′ UTR-impaired miR-19a/b effects. (**a** and **b**) Correlation of MXD1 expression with miR-19a (**a**) or miR-19b (**b**) expression in the 15 paired gastric cancer and normal tissues, totally 30 samples. The MXD1 expression was reversely correlated with miR-19a or miR-19b expression ($P = 0.001$ or $P = 0.009$, respectively). (**c**) Representative images of migrated cells on transwell plates that were originally plated with 5×10^4 gastric cancer cells transfected with pre-NC (NC), pre-miR-19a, pre-miR-19a and MXD1 without 3′UTR (pre-miR-19a + MXD1/ko), pre-miR-19b, pre-miR-19b and MXD1 without 3′UTR (pre-miR-19b + MXD1/ko). (**d**) The relative migration rate of A is indicated. Each experiment was repeated at least three times. Error bars correspond to the mean ± S.D. (*$P < 0.05$, *t*-test compared with the pre-miRNA group)

sequences of MXD1. Reintroducing MXD1 in cells impeded the migration, invasion and proliferation of gastric cancer cells and reduced the expression of miR-19a/b, while downregulating MXD1 by si-MXD1 promoted gastric cancer migration and invasion and increased miR-19a/b levels. These results indicate a unique mechanism by which a miRNA acts on a specific target within its multiple target pool to modulate specific responses.

Recently, miR-17-92 members have emerged as central players in networks that establish regulatory feedback circuits. Additionally, the targeted genes of this cluster are involved in distinct pathways so that the targeted gene may exert opposing effects. Several previous reports[5,26–28] confirmed that the E2F transcription factor family members can induce the expression of miR-17-92, and two of these family members are direct targets of miR-17-92, which generate a negative feedback loop aimed at restricting miR-17-92 transcription levels. In another report, Tili *et al.*[29] discovered that GAM reduces the transcriptional activation of the miR-17-92 promoter, downregulates miR-17-92 expression and limits the activation of genes related to the TGF-β canonical pathway. In contrast, TGF-β reduces GAM transcript levels while differentially upregulating miR-17-92 expression. In turn, miR-17-92 targeted GAM transcripts, thus establishing another auto-regulatory feedback loop. In the present study, despite the relationships between miR-19a/b and MXD1, we also found that c-Myc, the transactivator of miR-19a/b, can be reduced by introducing MXD1 into gastric cancer cells. Thus, the direct link between miR-19a/b miRNAs and the c-Myc antagonist gene MXD1 demonstrated a positive feedback loop between c-Myc, miR-19a/b and MXD1 that may be useful in reducing the opposite effects. Thus, auto-regulation contributes to the sustained induction of malignancies in gastric cancer.

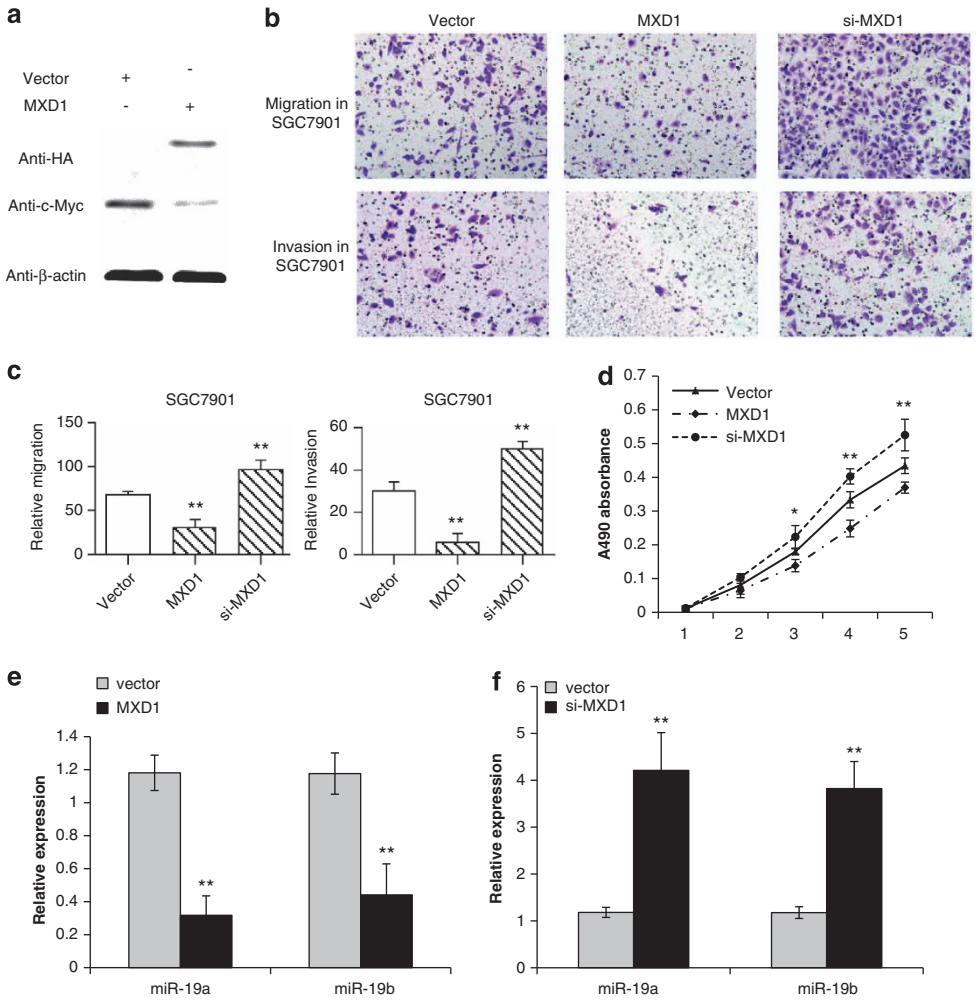

Figure 7 Overexpression of MXD1 repressed c-Myc and miR-19a/b levels and impeded the malignant phenotypes of gastric cancer cells. (**a**) Western blot of anti-HA and anti-c-Myc using HA-tagged MXD1 over-expressing cells and the vector control cells. (**b** and **c**) Effects of MXD1 in *in vitro* migration and invasion assays. (**b**) Representative pictures show effect of MXD1 and si-MXD1 on the migration and invasion of gastric cancer cells. (**c**) Quantification of migration and invasion assays of B (**$P \leq 0.01$ compared with the vector control). Each experiment was repeated at least three times. Error bars correspond to the mean ± S.D. (**d**) Effects of MXD1 on *in vitro* proliferation in gastric cancer (**$P \leq 0.01$, *$P \leq 0.05$, respectively, compared with the vector control). Each experiment was repeated at least three times. Error bars correspond to the mean ± S.D. (**e**) Real-time PCR show the expression levels of miR-19a and miR-19b in MXD1 over-expressing cells (**$P < 0.01$ compared with the vector control, *t*-test). Each experiment was independently repeated at least three times. Error bars correspond to the mean ± S.D. (**f**) Real-time PCR shows miR-19a and miR-19b expression levels in si-MXD1 expressing cells (**$P < 0.01$ compared with the vector control, *t*-test). Each experiment was independently repeated at least three times. Error bars correspond to the mean ± S.D.

As a last remark, the emergence of cancer coincides with a failure in regulating gene duplication, gene transcription and/or the levels of signalling molecules involved in regular metabolism. Therefore, it is possible that a new level of molecular complexity in tumours is generated by the development of robust genetic circuitries for the maintenance of cellular dysfunction and the prohibition of the organism to adapt to changing environments. MXD1, c-Myc and the miR-19a/b miRNAs have all been shown to increase in cancers; therefore, it is not surprising that they may be implicated in the control of cancer cell progression and tumour development and that they may interact with each other in different ways. Our study implied that the positive auto-regulatory network among miR-19a/b, MXD1 and c-Myc might be important in preserving the expression levels of oncogenic miRNAs and thus might provide a new viewpoint for the mechanism of the metastasis in gastric cancer.

Materials and Methods

Ethics statement. For the analysed tissue specimens, all patients gave informed consent to use excess pathological specimens for research purposes. The protocols employed in this study were approved by the hospital's Protection of Human Subjects Committee. The use of human tissues was approved by the institutional review board of the Fourth Military Medical University and conformed to the Helsinki Declaration, and to the local legislation. Patients offering samples for the study signed informed consent forms. In the animal experiments, all procedures for animal experimentation were performed in accordance with the Institutional Animal Care and Use Committee guidelines of the Experimental Animal centre of the Fourth Military Medical University. The approval ID for using the animals was No.12039 from Experimental Animal Centre of the Fourth Military Medical University.

Cell culture and reagents. The human gastric adenocarcinoma cell line SGC7901 was obtained from the Academy of Military Medical Science, and MKN28 was obtained from the Shanghai Cell Bank (Shanghai, China). These two cell lines were preserved in our institute. SGC7901Luc cells stably expressing firefly luciferase were generated and preserved in our lab. All of the cells were

grown in RPMI1640 (Invitrogen) supplemented with 10% heat-inactivated foetal calf serum (FCS) at 37 °C with 5% CO2 in a humidified incubator (Forma Scientific, Marietta, OH, USA). The precursors (pre-miRs) and inhibitors (miR-inhs) of the miRNAs miR-19a and miR-19b were obtained from Applied Biosystems (Invitrogen).

Construction of miR-19a and miR-19b lentivirus. For miR-19a and miR-19b sequences, two PCR primers were annealed to get the inserted sequences. The lentiviral vector pGCsil-H1 was double digested, purified and directly connected with the annealed products. The products were further transformed to competent bacterial cells for the growth of colonies, which were identified using PCR to get the positive clones. Positive clones identified by PCR were sequenced and analysed. Right clones were considered to be successfully constructed miR-19a and miR-19b plasmid lentiviral vectors. After ultrapure extraction to remove the endotoxin, the vectors were packaged with lentivirus into 293T cells using Lipofectamine 2000 (Invitrogen). Lentivirus was harvested and concentrated from cells and then titre was detected using GFP expressing strength.

Lentivirus miR-19a/b infection and stable cells. The lentiviral system with EGFP-expressing miR-19a (lenti-miR-19a) and miR-19b (lenti-miR-19b) and the negative control lenti-vector (lenti-NC) were purchased from Genechem (Shanghai Genechem Co., Ltd, Shanghai, China). Gastric cancer cell lines SGC7901, SGC7901Luc and MKN28 were infected with lenti-miR-19a, lenti-miR-19b or lenti-NC, according to the manufacturer's instructions, and stable cells were isolated by flow cytometry to sort EGFP-positive cells using flow cytometry.

Cell migration and invasion assays. Transwell migration and invasion assays were performed as described before.[30] The invasion assay was performed with Matrigel (BD Biosciences, Sparks, MD, USA) coated on the upper surface of the transwell chamber (Corning, Lowell, MA, USA). Cells that invaded or migrated through the membrane were fixed with methanol and stained with crystal violet. Photographs of four randomly selected fields of the fixed cells were taken and counted. Each experiment was repeated independently three times.

Animals and the *in vivo* metastasis assay. BALB/C nude mice at 4–6 weeks of age were handled using the best humane practices and cared for in accordance with NIH Animal Care Institutional Guidelines in the Experiment Animal Centre of the Fourth Military Medical University (Xi'an, Shaanxi Province, China). Firefly luciferase-labelled SGC7901 cells—SGC7901Luc were infected with lenti-miR-19a, lenti-miR-19b or lenti-NC, respectively, as described above, and stable clones were isolated. For *in vivo* metastasis assay, 2×10^6 cells were injected into the caudal veins of each nude mouse. Each group (miR-19a group, miR-19b group and NC group) contained six mice. After injection, bioluminescent signals were detected twice a week by the IVIS 100 Imaging System (Xenogen). Five minutes before imaging, the mice were injected intraperitoneally with 100 mg/kg D-luciferin. The mice were sacrificed seven weeks after injection of gastric cancer cells. For histological analysis, the lungs and livers of nude mice were harvested and fixed in 10% formalin before paraffin embedding, and then were sectioned and stained using H&E staining.

Reporter gene assay. For the reporter gene assay, cells were plated in 12-well plates and were transfected with 2 μg of MXD1 3′-UTR luciferase reporter plasmids (S) or the MXD1 3′-UTR antisense mutant (AS) and the empty pGL3-Control vector (Promega Biotech Co., Ltd, Beijing, China) using lipofectamine 2000 (Invitrogen). Cells were also cotransfected with the pre-miRNAs (150 nM, Applied Biosystems, Invitrogen). Assays were performed 24 h after transfection using the Dual Luciferase Reporter Assay system (Promega Biotech Co., Ltd). Firefly luciferase activities were normalised to Renilla luciferase activities. A miRNA precursor molecule control from Applied Biosystems (Invitrogen) was used as one of the negative miRNA controls and was referred to as pre-miR-NC. All experiments were performed in triplicate.

Western blot analysis. To determine the levels of protein expression, log phase cells were harvested from 90 mm culture plates, lysed in RIPA lysis buffer (150 mM NaCl, 50 mM Tris–HCl (pH 8.0), 0.1% SDS, 2 mM EDTA, 1 mM PMSF, 1% NP40, 5 μg/ml aprotinin and 1 μg/ml leupeptin) on ice, and then centrifuged at 12000 rpm for 10 min. Total proteins were resolved by 12% SDS-PAGE (Bio-Rad Laboratories, Inc., Hercules, CA, USA) and blotted onto nitrocellulose membranes (Amersham Biosciences Corp., Pittsburgh, PA, USA). Membranes were blocked with 10% non-fat milk powder at room temperature for 2 h and incubated overnight with primary antibodies: anti-MXD1 (1 : 1000; Abcam plc, Cambridge, MA, USA), anti-c-Myc (1 : 1000; Abcam plc) or anti-β-actin antibody (1 : 2000; Sigma-Aldrich Co., St. Louis, MO, USA). After three 5 min washes in triethanolamine-buffered saline solution with 0.1% Tween-20, membranes were incubated with horseradish peroxidase (HRP) conjugated secondary antibodies (1 : 2000; Santa Cruz biotechnology, Inc., Dallas, TX, USA) for 4 h at room temperature and then washed again in TBS-T and visualised with an enhanced chemi-luminescence kit (ECL-kit, Santa Cruz Biotechnology, Inc.). All experiments were performed in triplicate.

RNA extraction and quantitative real-time PCR (qRT-PCR). Total RNA from cancer tissues was extracted from FFPE-impeded tissue sections according to the manufacturer's instructions (AM1975, Applied Biosystems). Total RNA from cells was extracted using TRIZOL (Invitrogen), according to the manufacturer's instructions, with RNase-free DNase. Reverse transcription was performed according to the manufacturer's instructions (D350A, TaKaRa Biotechnology (DALIAN), Co., Ltd, DaLian, China). qRT-PCR was performed to determine the expression levels of each miRNA using the exact sequences (U–T) of these miRNAs as the forward primers and the unique q-PCR primer from the cDNA Synthesis Kit as the reverse primer. U6 was used as an internal control, and each plate contained one cDNA sample for each primer as a calibration sample. All experiments were performed in triplicate.

***In vitro* cell proliferation assay.** The *in vitro* cell proliferation assay was performed as described previously.[31] A total of 10^3 MXD1 (OriGene Technologies, Beijing, China) or si-MXD1 (Invitrogen) cells or cells transiently transfected with the control vector were used for the assays in 200 μl of complete medium. For proliferation of pre-miR-19a/b and miR-19a/b-inh, SGC7901 cells were used for transfection using pre-miRNAs, miRNA inhibitors and their negative controls, respectively. Twenty four hour later, cells were resuspended and 10^3 cells were used for the assays in 200 μl of complete medium. The cultures were assayed each day and read at a 490 nm absorbance (A490) on a micro-plate reader (168–1000 Model 680, Bio-Rad Laboratories, Inc.). Each experiment was performed in triplicate and repeated three times.

Statistical analysis. Continuous variables were compared by Student's *t*-test or an ANOVA test. If the test result of the homogeneity of variances between the groups was significant, the Mann–Whitney test was appropriately adopted. The χ^2-test or Fisher's test was used for categorical variables. The independent predictors of survival were calculated using the Cox regression model. The covariates incorporated into the multivariate analysis were the variables reaching $P < 0.05$ in an univariate analysis. Cumulative survival was assessed with Kaplan–Meier curves and compared using the log-rank test. Two-tailed *P*-values < 0.05 were considered statistically significant ($^*P < 0.05$; $^{**}P < 0.01$). All statistical analyses were conducted using SPSS software, version 14.0 (SPSS Inc., Chicago, IL, USA).

Conflict of Interest

The authors declare no conflict of interest.

Acknowledgements. This work was supported by National Basic Research Program of China (No. 2010CB732400, No.2010CB529300) and National Natural Science Foundation of China (No. 81172062, No. 81030044, No. 81000988).

1. Bartel DP. MicroRNAs: genomics, biogenesis, mechanism, and function. *Cell* 2004; **116**: 281–297.
2. Bartel DP. MicroRNAs: target recognition and regulatory functions. *Cell* 2009; **136**: 215–233.
3. Iliopoulos D, Jaeger SA, Hirsch HA, Bulyk ML, Struhl K. STAT3 activation of miR-21 and miR-181b-1 via PTEN and CYLD are part of the epigenetic switch linking inflammation to cancer. *Mol Cell* 2010; **39**: 493–506.
4. Calin GA, Croce CM. MicroRNA signatures in human cancers. *Nat Rev Cancer* 2006; **6**: 857–866.
5. O'Donnell KA, Wentzel EA, Zeller KI, Dang CV, Mendell JT. c-Myc-regulated microRNAs modulate E2F1 expression. *Nature* 2005; **435**: 839–843.

6. Castellano L, Giamas G, Jacob J, Coombes RC, Lucchesi W, Thiruchelvam P *et al.* The estrogen receptor-alpha-induced microRNA signature regulates itself and its transcriptional response. *Proc Natl Acad Sci USA* 2009; **106**: 15732–15737.
7. Hayashita Y, Osada H, Tatematsu Y, Yamada H, Yanagisawa K, Tomida S *et al.* A polycistronic microRNA cluster, miR-17-92, is overexpressed in human lung cancers and enhances cell proliferation. *Cancer Res* 2005; **65**: 9628–9632.
8. Lanza G, Ferracin M, Gafa R, Veronese A, Spizzo R, Pichiorri F *et al.* mRNA/microRNA gene expression profile in microsatellite unstable colorectal cancer. *Mol Cancer* 2007; **6**: 54.
9. Mestdagh P, Fredlund E, Pattyn F, Schulte JH, Muth D, Vermeulen J *et al.* MYCN/c-MYC-induced microRNAs repress coding gene networks associated with poor outcome in MYCN/c-MYC-activated tumors. *Oncogene* 2010; **29**: 1394–1404.
10. Mendell JT. miRiad roles for the miR-17-92 cluster in development and disease. *Cell* 2008; **133**: 217–222.
11. Mu P, Han YC, Betel D, Yao E, Squatrito M, Ogrodowski P *et al.* Genetic dissection of the miR-17 ~ 92 cluster of microRNAs in Myc-induced B-cell lymphomas. *Genes Dev* 2009; **23**: 2806–2811.
12. Olive V, Bennett MJ, Walker JC, Ma C, Jiang I, Cordon-Cardo C *et al.* miR-19 is a key oncogenic component of mir-17-92. *Genes Dev* 2009; **23**: 2839–2849.
13. Lin Q, Chen T, Lin G, Lin J, Chen G, Guo L. Serum miR-19a expression correlates with worse prognosis of patients with non-small cell lung cancer. *J Surg Oncol* 2013; **107**: 767–771.
14. Volinia S, Calin GA, Liu CG, Ambs S, Cimmino A, Petrocca F *et al.* A microRNA expression signature of human solid tumors defines cancer gene targets. *Proc Natl Acad Sci USA* 2006; **103**: 2257–2261.
15. Yao Y, Suo AL, Li ZF, Liu LY, Tian T, Ni L *et al.* MicroRNA profiling of human gastric cancer. *Mol Med Report* 2009; **2**: 963–970.
16. Guo J, Miao Y, Xiao B, Huan R, Jiang Z, Meng D *et al.* Differential expression of microRNA species in human gastric cancer versus non-tumorous tissues. *J Gastroenterol Hepatol* 2009; **24**: 652–657.
17. He L, Thomson JM, Hemann MT, Hernando-Monge E, Mu D, Goodson S *et al.* A microRNA polycistron as a potential human oncogene. *Nature* 2005; **435**: 828–833.
18. Song DW, Ryu JY, Kim JO, Kwon EJ, Kim do H. The miR-19a/b family positively regulates cardiomyocyte hypertrophy by targeting atrogin-1 and MuRF-1. *Biochem J* 2014; **457**: 151–162.
19. Xu XM, Wang XB, Chen MM, Liu T, Li YX, Jia WH *et al.* MicroRNA-19a and -19b regulate cervical carcinoma cell proliferation and invasion by targeting CUL5. *Cancer Lett* 2012; **322**: 148–158.
20. Hirao H, Jinnin M, Ichihara A, Fujisawa A, Makino K, Kajihara I *et al.* Detection of hair root miR-19a as a novel diagnostic marker for psoriasis. *Eur J Dermatol* 2013; **23**: 807–811.
21. Chen B, She S, Li D, Liu Z, Yang X, Zeng Z *et al.* Role of miR-19a targeting TNF-alpha in mediating ulcerative colitis. *Scand J Gastroenterol* 2013; **48**: 815–824.
22. Wu Q, Yang Z, Wang F, Hu S, Yang L, Shi Y *et al.* MiR-19b/20a/92a regulates the self-renewal and proliferation of gastric cancer stem cells. *J Cell Sci* 2013; **126**(Pt 18): 4220–4229.
23. Wang F, Li T, Zhang B, Li H, Wu Q, Yang L *et al.* MicroRNA-19a/b regulates multidrug resistance in human gastric cancer cells by targeting PTEN. *Biochem Biophys Res Commun* 2013; **434**: 688–694.
24. Ayer DE, Kretzner L, Eisenman RN. Mad: a heterodimeric partner for Max that antagonizes Myc transcriptional activity. *Cell* 1993; **72**: 211–222.
25. Chin L, Schreiber-Agus N, Pellicer I, Chen K, Lee HW, Dudast M *et al.* Contrasting roles for Myc and Mad proteins in cellular growth and differentiation. *Proc Natl Acad Sci USA* 1995; **92**: 8488–8492.
26. Dews M, Homayouni A, Yu D, Murphy D, Sevignani C, Wentzel E *et al.* Augmentation of tumor angiogenesis by a Myc-activated microRNA cluster. *Nat Genet* 2006; **38**: 1060–1065.
27. Sylvestre Y, De Guire V, Querido E, Mukhopadhyay UK, Bourdeau V, Major F *et al.* An E2F/miR-20a autoregulatory feedback loop. *J Biol Chem* 2007; **282**: 2135–2143.
28. Woods K, Thomson JM, Hammond SM. Direct regulation of an oncogenic micro-RNA cluster by E2F transcription factors. *J Biol Chem* 2007; **282**: 2130–2134.
29. Tili E, Michaille JJ, Liu CG, Alder H, Taccioli C, Volinia S *et al.* GAM/ZFp/ZNF512B is central to a gene sensor circuitry involving cell-cycle regulators, TGF{beta} effectors, Drosha and microRNAs with opposite oncogenic potentials. *Nucleic Acids Res* 2010; **38**: 7673–7688.
30. Tie J, Pan Y, Zhao L, Wu K, Liu J, Sun S *et al.* MiR-218 inhibits invasion and metastasis of gastric cancer by targeting the Robo1 receptor. *PLoS Genet* 2010; **6**: e1000879.
31. Wu Q, Jin H, Yang Z, Luo G, Lu Y, Li K *et al.* MiR-150 promotes gastric cancer proliferation by negatively regulating the pro-apoptotic gene EGR2. *Biochem Biophys Res Commun* 2010; **392**: 340–345.

Supplementary Information accompanies this paper on Cell Death and Disease website (http://www.nature.com/cddis)